Supporting text 1: Formulation of the clumped self-shielding in self-shielding

In Section “Calculations of self-shielding using synthesized absorption spectra”, we used the ${}^{2A,2B}\gamma$ value as a fractionation factor of clumped isotopes as follows:

$$ {}^{2A,2B}\gamma = ({}^{2A,2B}J \times {}^{1A,1B}J)/({}^{2A}J \times {}^{2B}J) \quad (10) $$

In the case where four each isotopologue absorbs a different wavelength (Fig. 1B), the rate constants are

$$ {}^{xA,xB}J = \sigma\Delta\lambda \exp(- {}^{xA,xB}N\rho'\sigma) = \sigma\Delta\lambda \exp(-\tau\, {}^{xA,xB}N) \quad (S1) $$

$$ (\text{i.e., } {}^{1A,1B}J = \sigma\Delta\lambda \exp(-\tau\, {}^{1A,1B}N) \text{ and } {}^{2A,2B}J = \sigma\Delta\lambda \exp(-\tau\, {}^{2A,2B}N)\ ) $$

$$ {}^{2A}J = {}^{1B}N\, {}^{2A,1B}J + {}^{2B}N\, {}^{2A,2B}J = \sigma\Delta\lambda\, [{}^{1B}N \exp(-\tau\, {}^{2A,1B}N) + {}^{2B}N \exp(-\tau\, {}^{2A,2B}N)] \quad (S2) $$

$$ {}^{2B}J = {}^{1A}N\, {}^{1A,2B}J + {}^{2A}N\, {}^{2A,\,B}J = \sigma\Delta\lambda\, [{}^{1A}N \exp(-\tau\, {}^{1A,2B}N) + {}^{2A}N \exp(-\tau\, {}^{2A,2B}N)] \quad (S3) $$

where ${}^{2A}N$, ${}^{2B}N$, and ${}^{xA,xB}N$ represent abundances of ^{2}AB (a sum of ${}^{2}A{}^{1}B$ and ${}^{2}A{}^{2}B$), $A{}^{2}B$ (a sum of ${}^{1}A{}^{2}B$ and ${}^{2}A{}^{2}B$),${}^{x}A{}^{x}B$ isotopologues, respectively. To capture rough trend, when absorptions by minor isotopologues (${}^{2}A{}^{1}B$, ${}^{1}A{}^{2}B$, and ${}^{2}A{}^{2}B$) are ignored and ${}^{1A,1B}N$ is assumed to be 1, Eqs. (S1)−(S3) are approximated as follows:

$$ {}^{1A,1B}J \approx \sigma\Delta\lambda e^{-\tau} \quad (S4) $$

$$ {}^{2A,2B}J \approx \sigma\Delta\lambda \quad (S5) $$

$$ {}^{2A}J \approx \sigma\Delta\lambda\ ({}^{1B}N + {}^{2B}N) \quad (S2') $$

$$ {}^{2B}J \approx \sigma\Delta\lambda\ ({}^{1A}N + {}^{2A}N) \quad (S3') $$

Here, ${}^{1B}N + {}^{2B}N$ and ${}^{1A}N + {}^{2A}N$ are equal to 1. Thus, the J values are

$$ {}^{2A}J \approx \sigma\Delta\lambda \quad (S2'') $$

$$ {}^{2B}J \approx \sigma\Delta\lambda \quad (S3'') $$

leading to ${}^{2A,2B}\gamma \approx e^{-\tau}$ (main text).

On the other hand, the Rayleigh fractionation for clumped isotope was formulated by Whitehill et al. (2017) in their Section A.2 as follows:

$$ \Delta \approx \Delta_0 + 1000\, [{}^{2A}\varepsilon\, {}^{2B}\varepsilon + ({}^{2A,2B}\gamma - 1)\, {}^{2A}\alpha\, {}^{2B}\alpha] \times \ln f\ ‰ \quad (S6) $$

where f is the remaining fraction, Δ is the clumped isotope composition at a remaining fraction of f, and Δ_0 is the initial clumped isotope composition. Alfa and epsilon values are

$$ {}^{2A}\alpha = {}^{2A}J/{}^{1A}J \quad (S7) $$

$$ {}^{2B}\alpha = {}^{2B}J/{}^{1B}J \quad (S8) $$

$$ {}^{2A}\varepsilon = {}^{2A}\alpha - 1 \quad (S9) $$

$$ {}^{2B}\varepsilon = {}^{2B}\alpha - 1 \quad (S10) $$

${}^{1A}J$ and ${}^{1B}J$ are

$$ {}^{1A}J = {}^{1A}N\, {}^{1A,1B}J + {}^{2B}N\, {}^{1A,2B}J = \sigma\Delta\lambda\, [{}^{1A}N \exp(-\tau\, {}^{1A,1B}N) + {}^{2B}N \exp(-\tau\, {}^{1A,2B}N)] \quad (S11) $$

$$ {}^{1B}J = {}^{1B}N\, {}^{1A,1B}J + {}^{1A}N\, {}^{2A,1B}J = \sigma\Delta\lambda\, [{}^{1B}N \exp(-\tau\, {}^{1A,1B}N) + {}^{2A}N \exp(-\tau\, {}^{2A,1B}N)] \quad (S12) $$

When the τ is ~1 and ${}^{1A}N$ is 1 and minor isotopes are ignored (i.e., ${}^{1A}N >> {}^{2B}N$ and ${}^{1B}N$

>> ${}^{2A}N$), ${}^{1A}J$ and ${}^{1B}J$ are

$$ {}^{1A}J \approx \sigma \Delta \lambda {}^{1A}N \exp(-\tau\, {}^{1A,1B}N) \quad \text{(S11')} $$

$$ {}^{1B}J \approx \sigma \Delta \lambda {}^{1B}N \exp(-\tau\, {}^{1A,1B}N) \quad \text{(S12')} $$

Moreover, assuming that are ${}^{1A}N$, ${}^{1B}N$, and ${}^{1A,1B}N$ are 1, ${}^{1A}J$ and ${}^{1B}J$ are

$$ {}^{1A}J \approx \sigma \Delta \lambda e^{-\tau} \quad \text{(S11'')} $$

$$ {}^{1B}J \approx \sigma \Delta \lambda e^{-\tau} \quad \text{(S12'')} $$

Finally, substituting Eqs. (S7)−(S10), (S2”), (S3”), (S11”), and (S12”) for Eq. (S6) leads to Eq. (12) in the main text

$$ \Delta \approx \Delta_0 + 1000\,(1-e^{\tau}) \times \ln f \text{‰} \quad (12) $$

Supporting text 2: Estimation of total pressure dependence under pure SO_2 atmosphere

Some SO_2 photolysis experiments were conducted under pure SO_2 atmospheres. For comparing this study with previous studies, SO_2 self-broadening coefficient is useful. However, the self-pressure broadening coefficient of SO_2 in the C band is unknown. These coefficients are likely larger than N_2 broadening coefficients because of polarity SO_2. For example, line by line SO_2 coefficients have been reported at 9.2 μm (IR region), the self-broadening coefficients are about 3-4 times of those of N_2 (Tasinato et al., 2010, 2014). Moreover, the HITRAN database (Gordon et al., 2017) presents 18,948 pairs of self and air (80% N_2 and 20% O_2) broadening coefficients of SO_2 ranging from 0.17 to 116 cm^{-1} (Sumpf et al., 1996a, 1996b, 1997; Ball et al., 1996; Kühnemann et al., 1992; Cazzoli and Puzzarini, 2012; Tasinato et al., 2013, 2014). Although the self-broadening coefficients depend on the rotational excitation quantum number, the average between self-broadening and air broadening coefficients ratios is 3.61 and the standard deviation is 1.06. When we apply the ratio into the C band, the pressure broadening coefficient of SO_2 may possibly approach ~1 cm^{-1} bar^{-1}.

In Figs. 6 and 7, 0.90 cm^{-1} bar^{-1}, which is 3 times of N_2 broadening coefficient, is assumed as SO_2 self-broadening coefficient.

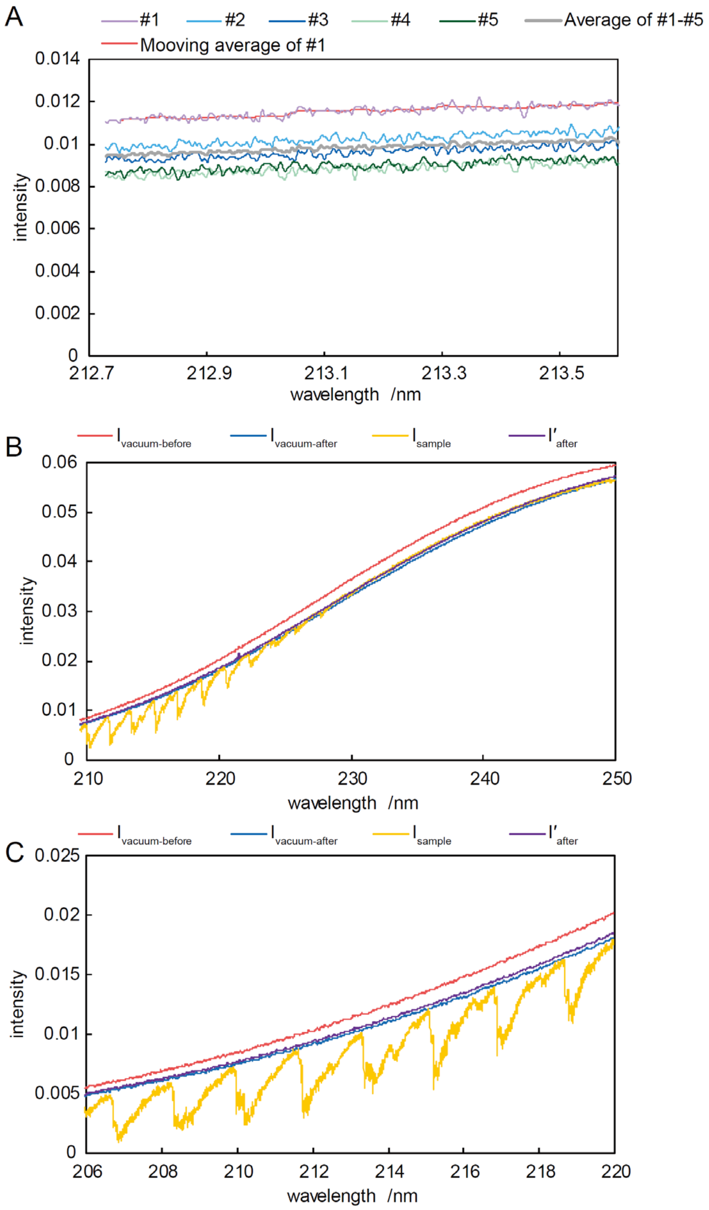

Fig. S1. An approach to reduce uncertainties induced by noise and drift effects. Examples of I_{vacuum} calibrations. (A) Typical raw data of I_{vacuum} (#1-#5), average of #1-#5 (gray), and moving average of #1 (red). Magnitudes variates in #1-#5. Because average from #1 to #5 is smoother than each raw data, variation of signals seems random. Thus, it is reasonable that moving average is used to decrease errors. Points of moving average are optimized, and moving averages of 41 points (red line) were used. (B) Calibration of signals of change over time. At 235-245 nm where the amplitude of SO_2 absorption is small, I_{sample} is located between $I_{\text{vacuum-before}}$ and $I_{\text{vacuum-after}}$, which are measured just before and just after. A purple line is the best fit line by eq. (1). Panel (C) is a zoom of panel (B) from 206 to 220 nm.

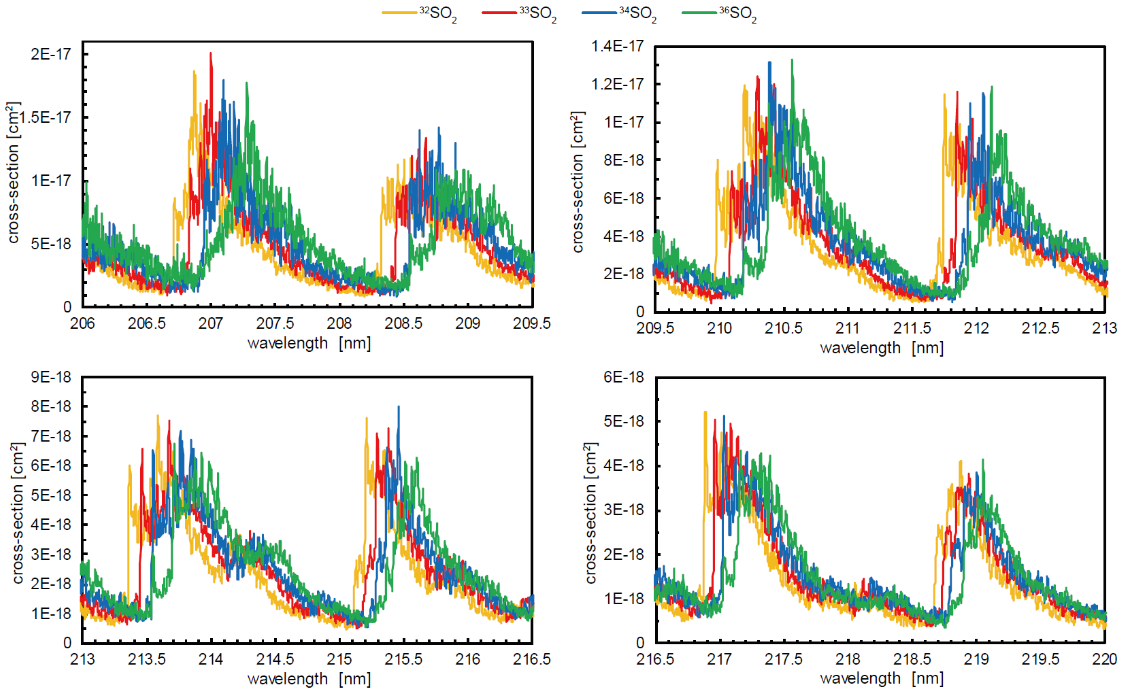

Fig. S2. Comparison of measured $^{32,33,34,36}SO_2$ absorption cross-sections. Isotope shift at shorter wavelength is larger than longer wavelength, shown as Danielache et al. (2008). Note that vertical scales are different between panels.

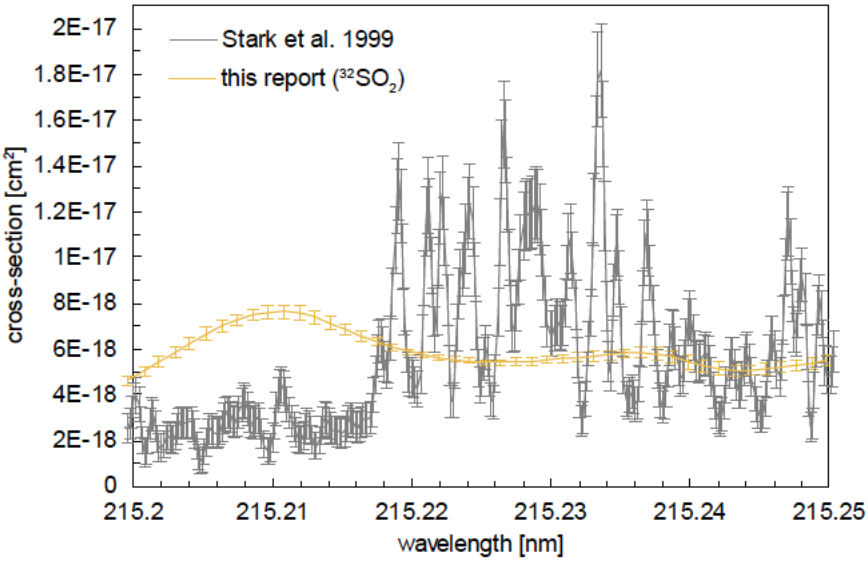

Fig. S3. Comparison between data presented in this report and error bars added spectra reported by Stark et al. (1999). The embedded figure shows the relative error of the spectra in this report at each wavelength in the 215.2-215.25 nm spectral range.

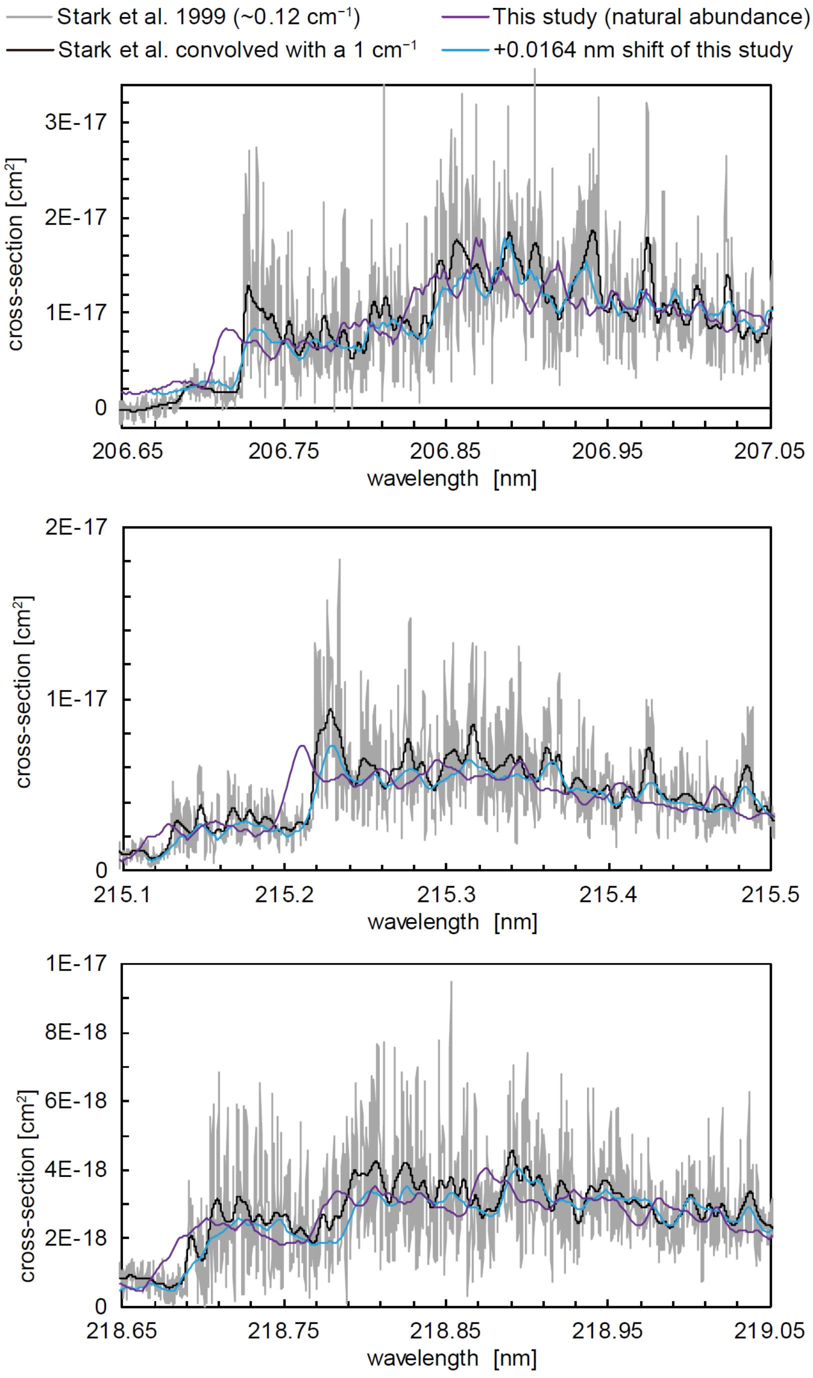

Fig. S4. Comparison between data presented in this report of natural abundance of sulfur isotopes and convolved spectra reported by Stark et al. (1999). Gray lines represent original data of Stark et al. (1999), black lines represent convolved data from Stark et al. (1999), purple lines represent natural abundance SO_2 spectra of this study, and a light blue line is 4.0984 cm^{-1} (17 wavenumber steps, ~0.0164 nm) wavelength shift from natural abundance SO_2 spectra of this study. The natural abundance of sulfur isotopes is $^{32}S/^{33}S/^{34}S/^{36}S=95.018/0.75/4.215/0.017$.

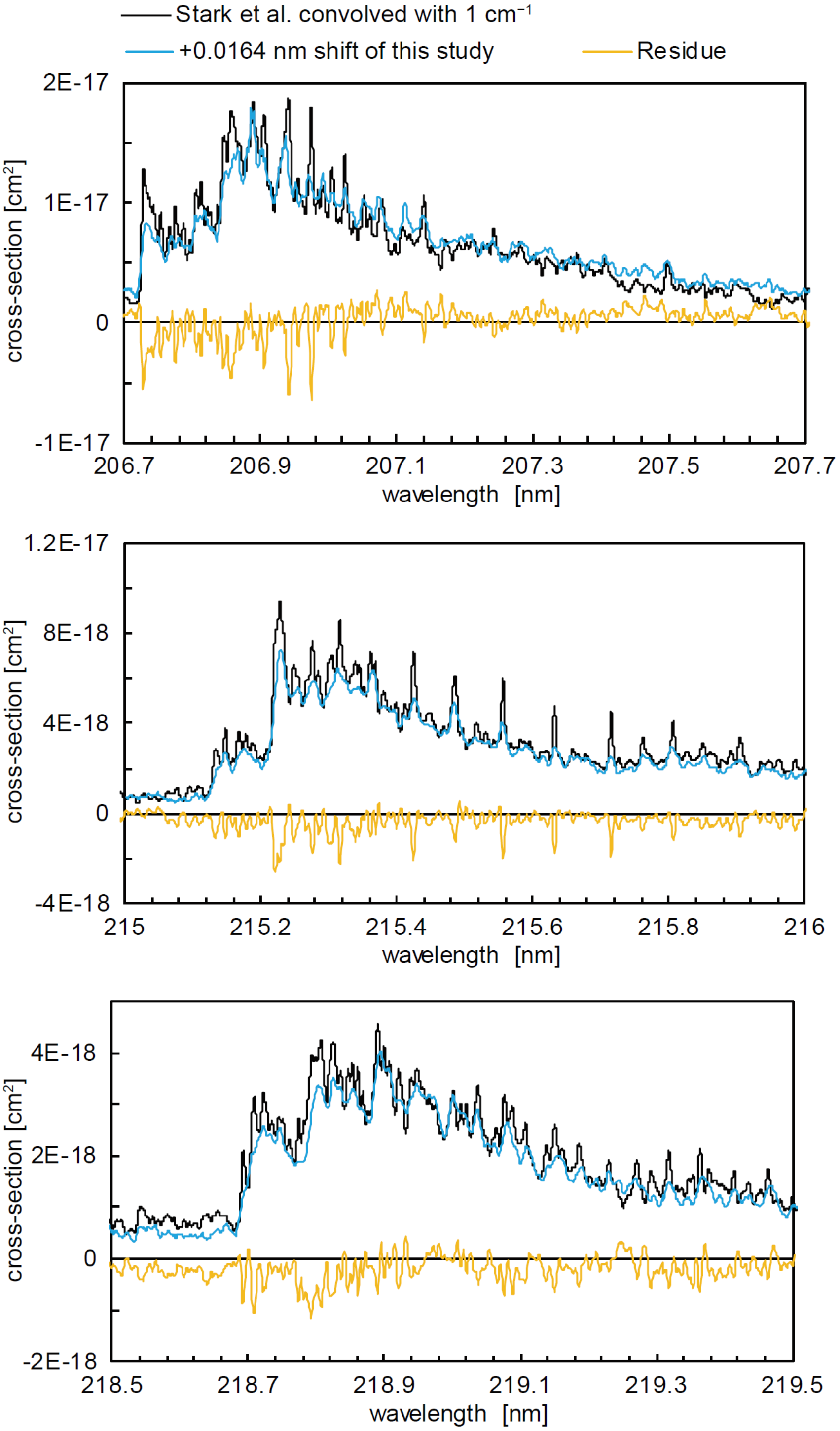

Fig. S5. Comparison between data presented in this report of 4.0984cm^{-1} (~0.0164 nm) shift (blue lines) and convolved spectra reported by Stark et al. (1999) (black lines). Yellow lines represent residue, which is magnitudes of shifted cross-section of this study minus convolved cross-section of Stark et al. (1999).

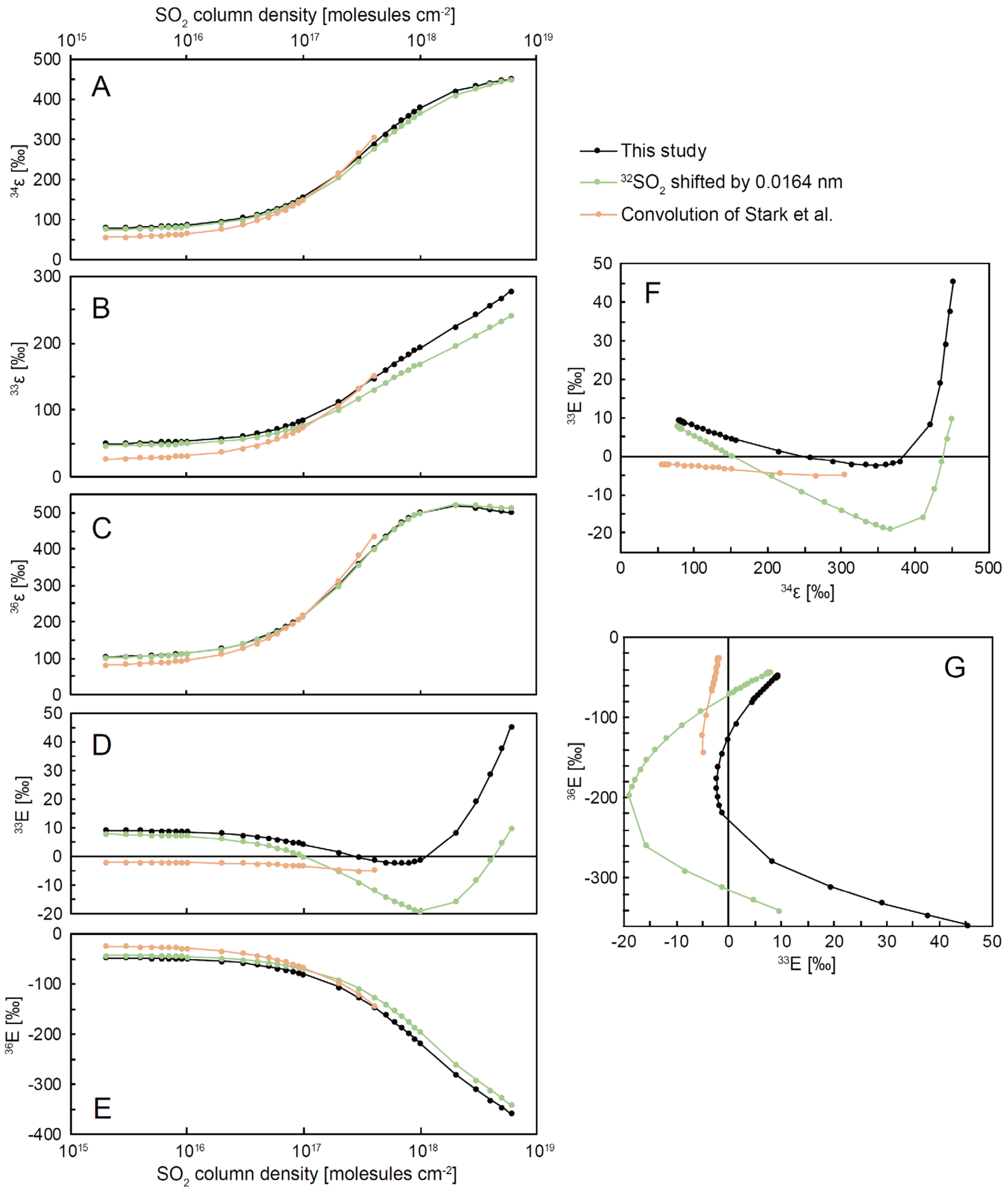

Fig. S6. Calculated fractionation factors by SO_2 isotopologues absorption cross-sections. Plots of ((A) $^{34}\varepsilon$, (B) $^{33}\varepsilon$, (C) $^{36}\varepsilon$, (D) ^{33}E, and (E) ^{36}E) vs. SO_2 column density, (F) $^{34}\varepsilon$ vs ^{33}E), and (G) ^{33}E vs ^{36}E. Black lines represent this study (same as black lines in Fig. 5). Light green lines represent wavelength uncertainty, that is, $^{32}SO_2$ absorption spectra were shifted of 4.0984 cm^{-1} (~0.0164 nm). Orange lines represent uncertainty of cross-section magnitude, that is, $^{32}SO_2$ absorption spectra is assumed as 1 cm^{-1} convolution of Stark et al. (1999).